



**HAL**  
open science

## First Results on $^{238}\text{U}(n,f)$ Prompt Fission Neutron Spectra from 1 to 200 MeV incident neutron energy

Paola Marini, Benoit Laurent, Gilbert Belier, Thomas Bonnet, Audrey Chatillon, Julien Taieb, David Etasse, Matthew Devlin, Robert Haight

► **To cite this version:**

Paola Marini, Benoit Laurent, Gilbert Belier, Thomas Bonnet, Audrey Chatillon, et al.. First Results on  $^{238}\text{U}(n,f)$  Prompt Fission Neutron Spectra from 1 to 200 MeV incident neutron energy. 6th Workshop on Nuclear Fission and Spectroscopy of Neutron-Rich Nuclei, Mar 2017, Chamrousse, France. pp.03002, 10.1051/epjconf/201819303002 . hal-04529750

**HAL Id: hal-04529750**

**<https://hal.science/hal-04529750>**

Submitted on 24 May 2024

**HAL** is a multi-disciplinary open access archive for the deposit and dissemination of scientific research documents, whether they are published or not. The documents may come from teaching and research institutions in France or abroad, or from public or private research centers.

L'archive ouverte pluridisciplinaire **HAL**, est destinée au dépôt et à la diffusion de documents scientifiques de niveau recherche, publiés ou non, émanant des établissements d'enseignement et de recherche français ou étrangers, des laboratoires publics ou privés.



Distributed under a Creative Commons Attribution 4.0 International License

# First Results on $^{238}\text{U}(\text{n},\text{f})$ Prompt Fission Neutron Spectra from 1 to 200 MeV incident neutron energy

Paola Marini<sup>1,\*</sup>, Benoit Laurent<sup>1</sup>, Gilbert Belier<sup>1</sup>, Thomas Bonnet<sup>1</sup>, Audrey Chatillon<sup>1</sup>, Julien Taieb<sup>1</sup>, David Etasse<sup>2</sup>, Matthew Devlin<sup>3</sup>, and Robert Haight<sup>3</sup>

<sup>1</sup>CEA, DAM, DIF, F-91297 Arpajon, France

<sup>2</sup>LPC Caen, ENSICAEN, Université de Caen, CNRS/IN2P3, Caen, France

<sup>3</sup>P-27, Los Alamos National Laboratory, Los Alamos, NM-87544, USA

**Abstract.** A new  $^{238}\text{U}(\text{n},\text{f})$  prompt fission neutron spectra (PFNS) measurement has been recently performed at the WNR facility of the Los Alamos National Laboratory. The measurement allows one to explore the dependence of the prompt fission neutron energy spectra on the incident neutron energy. The experimental setup couples the Chi-Nu scintillator array to a newly developed fission chamber, characterized by an improved alpha-fission discrimination and time resolution, a reduced amount of matter in the neutron beam and a higher actinide mass. The dedicated setup and the high statistics collected allow us to obtain a good precision on the measured fission neutron energy, as well as to explore the low energy region, down to 650keV, and the high energy region, above 5 MeV, of the emitted neutron spectrum. These are indeed the regions where discrepancies in the evaluated PFNS data are found. We present here the first preliminary results of the experiment.

## 1 Introduction

Prompt fission neutron spectra (PFNS) provide valuable information for the understanding of the fission process and represent a key parameter for nuclear energy applications.

The experimental database of fission neutron spectra collects few data, far less precise than those on the other fission observables, and presents significant discrepancies especially below 1 MeV and above 5 MeV. From a theoretical point of view, microscopic models of fission still do not provide reliable predictions, therefore evaluated PFNS are obtained from phenomenological models. To test and validate these models and improve data for applications, precise PFNS measurements are required.

Our group, involved since 2000's in PFNS measurements [1–3], has done a special effort to improve the accuracy by developing new dedicated tools. We describe here the last experiment that we performed on  $^{238}\text{U}$  PFNS.

## 2 The experiment

The experiment was carried out at the WNR facility [4, 5] at the Los Alamos National Laboratory, where a white pulsed neutron beam, spanning an energy range from below 1 MeV to several hundreds

---

\*e-mail: [paola.marini@cea.fr](mailto:paola.marini@cea.fr)

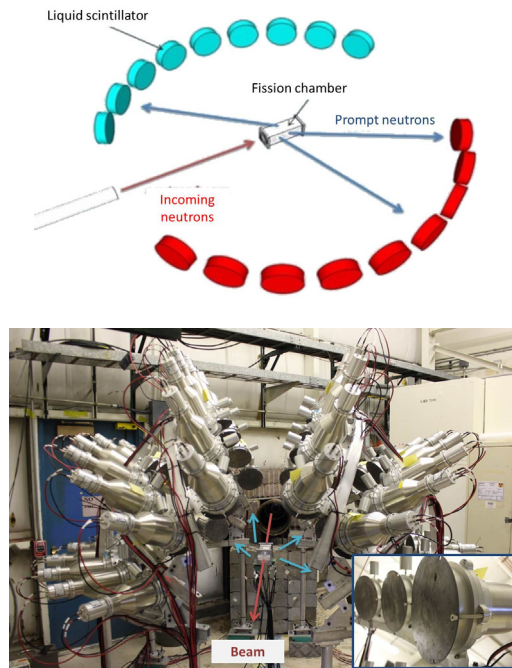


**Figure 1.** a) Schematic view of the setup on the beam-fission chamber plane. Neutron detectors out of the horizontal plane are not shown. b) Photo of the setup.

of MeV, is produced by 800 MeV proton-induced spallation reactions on a tungsten target. The neutron beam is collimated along a flight path of 20 m before impinging on to the actinide target under study.

The experimental setup, sketched in Fig. 1a), couples the 54 Chi-Nu scintillator array [6] to a newly developed fission chamber [7] and a numerical DAQ. A photo of the setup is shown in Fig. 1b).

### *Fission chamber*

The fission chamber was conceived to contain 360 mg of  $^{238}\text{U}$  arranged in 72 deposits in the chamber. The uranium was deposited on both sides of the anodes and cathodes of the chamber. An identical chamber, containing a  $^{252}\text{Cf}$  deposit, was also used for neutron detection efficiency measurements. The properly chosen gap distance of 2.5 mm between each anode and cathode of the chamber allowed to obtain an improved  $\alpha$ -fission fragment discrimination, with a fission detection efficiency better than 95%. Two pulse height spectra (shown in Fig. 2) measured during the experiment with (in red) and without (in blue) beam illustrate the achieved  $\alpha$ -fission fragment discrimination. The reduced amount of structural material reduced the neutrons scattering both from the incoming neutron beam and from the emitted fission neutrons. Dedicated pre-amplifiers were developed to match the detector characteristics and achieve a time resolution less than 0.8 ns FWHM. This lead to a time-of-flight resolution for the incident and emitted neutrons of about 1.5 ns. The latter arises from the fission-chamber time resolution and the proton-bunch width for the incident neutrons, and from the fission-chamber and the scintillator-photomultiplier time resolution for the emitted neutrons. A more detailed description of the fission chamber can be found in [7].

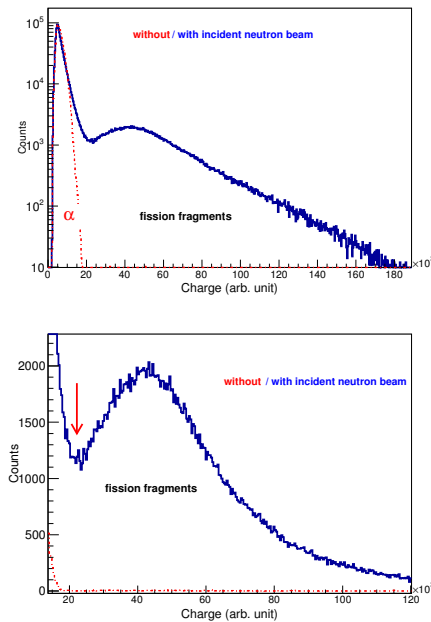


**Figure 2.** Pulse height spectra of  $^{238}\text{U}$  fission chamber in logarithmic (a) and linear (b) scale.

### Neutron detection array

The Chi-Nu array is constituted by 54 EJ-309 liquid scintillator cells, read by photomultipliers, and arranged on a half-sphere with radius about 1 m around the fission chamber, as shown in Fig.1. The detectors cover about 10% of the solid angle, and are placed at different angles, from  $30^\circ$  to  $150^\circ$ , with respect to the beam axis, allowing to study the angular distribution of the emitted neutrons.

The EJ-309 scintillator, sensitive to both neutrons and  $\gamma$  rays, allows their discrimination via Pulse Shape Discrimination (PSD) technique. The latter is based on the charge integration of the long and short components of the pulse. The amount of  $\gamma$  rays impinging on the cells was reduced by placing a Pb shield in front of each cell. A typical pulse-shape discrimination plot is shown in Fig.3, where the long to short pulse-component ratio (PSD) is plotted as a function of the total pulse charge.

### Data acquisition system

The FASTER digital acquisition system [8] was used during the experiment. Signals were digitalized by a 500 MHz, 12-bits, low noise Analog to Digital Converter (ADC) and processed by real time numerical modules implemented on FPGAs (Field Programmable Gate Array). The signal over noise ratio, as well as the zero time crossing determination on the Constant Fraction discriminator signal, are optimized by limiting the analog bandwidth by the use of an input passive low pass filter (100 MHz). Time data with 7.8 ps accuracy can be provided by FASTER. The accepted counting rate is as high as 700 kHz. The use of this acquisition system allowed us to avoid numerical dead-time. Moreover, thanks to the very low noise level, low neutron detection thresholds ( $\sim 500$  keV) could be set on the scintillators.

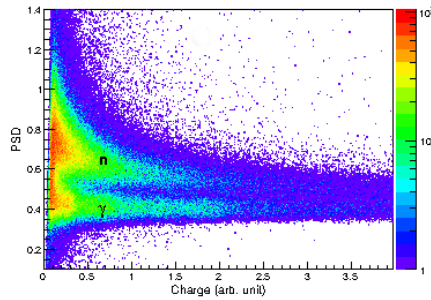


**Figure 3.** Pulse shape discrimination vs total charge deposited in a cell by  $\gamma$  rays and neutrons.

### 3 Data analysis and preliminary results

The experiment takes advantage of the double time-of-flight technique. For each triggered event, the time of flight of the incoming neutron from the spallation target to the fission chamber and the time of flight of the emitted neutron from the fission chamber to the scintillator were measured. This gives us access to the incident and emitted neutron kinetic energies.

A threshold to discriminate fission from  $\alpha$  decay events was set in the fission chamber (see Fig.2).

Special efforts were made to improve the  $\gamma$ -neutron discrimination and  $\gamma$  ray rejection, taking advantage both of the pulse shape discrimination and of the scintillator light output vs deposited energy correlations.

The neutron detector efficiencies were obtained by measuring the PFNS of the  $^{252}\text{Cf}$  spontaneous fission in the same experimental conditions. The efficiencies are determined with respect to the Manhart evaluated standard [9] and applied to the data. Dedicated efficiency measurements are planned to implement possible corrections.

The presence of structural and surrounding materials causes the scattering of neutrons, introducing a background in the PFNS which must be subtracted. The first component of background is represented by scattered incident neutrons. This background is not correlated to fission events and was measured by triggering on  $\alpha$  events and analyzing the random coincidences in the neutron detectors. A second component of background comes from the scattering of prompt fission neutrons, which leads to an erroneous determination of their kinetic energy. This contribution is accounted for, at a first order, when correcting the spectra for the detector efficiency. Indeed the efficiency measurement was performed in the same experimental conditions as the real measurement. Moreover, under the assumption that the  $^{252}\text{Cf}$  and  $^{238}\text{U}$  have similar PFNS, the distortions due to the scattering are similar.

Thanks to the high statistics which was accumulated during the experiment and the low detection thresholds, the evolution of the observables can be studied as a function of the incident neutron energy between 0.8 and 200 MeV. In Fig.4 the preliminary PFNS obtained for 5 to 6 and 7 to 8 MeV incident neutron energy bins are presented, showing the high precision attained in the measurement, which is sensitive to evaporated neutrons from  $2^{nd}$ -chance fission. The precise determination of the PFNS shape as a function of the incident energy allows to test models for the high energy part of the spectrum, which might be too hard in the current evaluations [10]. Also a precise ( $< 0.2\%$ ) estimation of the mean fission neutron energy can be obtained, which is an indirect measurement of the nuclear temperature. Within a Fermi gas approach, currently used fission models describe the nuclear level density as dependent on the nuclear temperature. This is not the case for a recent fission model [11–

13] which proposes a constant temperature level density. Our data could help in testing these models. Finally the high angular coverage and granularity will allow us to investigate possible angular dependence of the fission neutrons and the evolution of the neutron multiplicity with the incident neutron energy.

The analysis is currently ongoing and final and complete results will be published in forthcoming publications.

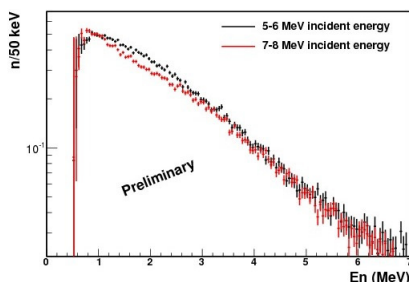


**Figure 4.** Preliminary  $^{235}\text{U}(n,f)$  PFNS for 5 to 6 and 7 to 8 MeV incident energy bins. Only a part of the statistics is presented.

## 4 Conclusions

We have presented the very preliminary results on the measurement of  $^{238}\text{U}$  PFNS. The dedicated setup couples a newly developed fission chamber to a high angular coverage neutron detector array and a digital acquisition system. This allows one to obtain a high statistics with very low detection thresholds and therefore to study different observables as a function of the incident neutron energy.

## References

- [1] T. Ethvignot, M. Devlin, R. Drog, T. Granier, R. Haight, B. Morillon, R. Nelson, J. O'Donnell, D. Rochman, *Physics Letters B* **575**, 221 (2003)
- [2] A. Chatillon, G. Bélier, T. Granier, B. Laurent, B. Morillon, J. Taieb, R.C. Haight, M. Devlin, R.O. Nelson, S. Noda et al., *Phys. Rev. C* **89**, 014611 (2014)
- [3] J. Taieb, T. Granier, T. Ethvignot, M. Devlin, R. Haight, R. Nelson, J. O'Donnell, D. Rochman, in *Proceedings of the International Conference on Nuclear Data for Science and Technology* (2007), p. 429
- [4] P. Lisowski, C. Bowman, G. Russell, S. Wender, *Nucl. Sci. Eng.* **106**, 208 (1990)
- [5] P.W. Lisowski, K.F. Schoenberg, *Nucl. Instr. and Meth. A* **562**, 910 (2006)
- [6] R.C. Haight, H.Y. Lee, T.N. Taddeucci, J.M. O'Donnell, B.A. Perdue, N. Fotiades, M. Devlin, J.L. Ullmann, A. Laptev, T. Bredeweg et al., *Journal of Instrumentation* **7**, C03028 (2012)
- [7] J. Taieb, B. Laurent, G. Bélier, A. Sardet, C. Varignon, *Nucl. Instr. and Meth. A* **833**, 1 (2016)
- [8] FASTER, *LPC-Caen* (2013), <http://faster.in2p3.fr>
- [9] W. Mannhart, *TECDOC-410, IAEA, Vienna, 158*, in *Proceedings of the IAEA Advisory Group Mett. Properties of Neutron Sources* (1987)

- [10] M. Chadwick, M. Herman, P. Obložinský, M. Dunn, Y. Danon, A. Kahler, D. Smith, B. Pritychenko, G. Arbanas, R. Arcilla et al., Nuclear Data Sheets **112**, 2887 (2011), Special Issue on ENDF/B-VII.1 Library
- [11] K.H. Schmidt, B. Jurado, Phys. Rev. Lett. **104**, 212501 (2010)
- [12] K.H. Schmidt, B. Jurado, Phys. Rev. C **83**, 014607 (2011)
- [13] K.H. Schmidt, B. Jurado, Phys. Rev. C **83**, 061601 (2011)